# Integrating the Gradient of the Thin Wire Kernel

Nathan J. Champagne(1) and Donald R. Wilton(2)
(1) ESCG, Houston, TX 77258–8477, USA
(2) University of Houston, Houston, TX 77204–4005, USA

## Introduction

When the source and observation points are close, the potential integrals over wire segments involving the wire kernel are split into parts to handle the singular behavior of the integrand [1]. The singularity characteristics of the gradient of the wire kernel are different than those of the wire kernel, and the axial and radial components have different singularities. The characteristics of the gradient of the wire kernel are discussed in [2].

## Integration of the Gradient of the Wire Kernel

To evaluate the near electric and magnetic fields of a wire, the integration of the gradient of the wire kernel needs to be calculated over the source wire. Since the vector bases for current have constant direction on linear wire segments, these integrals reduce to integrals of the form

$$\begin{aligned}\int_{z_L}^{z_U} & B(\xi_1,\xi_2)\nabla K(\rho,z-z')\,dz' \\ &= \left[\int_{z_L}^{z-\Delta z_1}+\int_{z-\Delta z_1}^{z}+\int_{z}^{z+\Delta z_2}+\int_{z+\Delta z_2}^{z_U}\right] B(\xi_1,\xi_2)\nabla K(\rho,z-z')\,dz' \\ &= I_1+I_2+I_3+I_4,\end{aligned} \tag{1}$$

where $B(\xi_1,\xi_2)$ is a basis function in normalized segment variables $\xi_1$, $\xi_2=1-\xi_1$ for scalar current, $\nabla K(\rho,z-z')$ is the gradient of the wire kernel, $z$ is the projection of the observation point onto the wire, $\rho$ is the perpendicular distance from the wire axis to the observation point, and $\Delta z_1$ and $\Delta z_2$ are defined as in [1].

On the wire surface, the gradient of the wire kernel $\nabla K(\rho,z-z')$ is dominated by a near-delta function behavior in a neighborhood ($\Delta z_1$ and $\Delta z_2$) about the projection of the observation point onto the segment $\left(\xi_1^0,\xi_2^0\right)$ [2]. The integrals $I_2$ and $I_3$ are designed to account for this behavior. Outside this neighborhood, the gradient of the wire kernel has a $1/R^3$ behavior that is treated in $I_1$ and $I_4$.

The first integral,

$$I_1=\int_{z_L}^{z-\Delta z_1} B(\xi_1,\xi_2)\nabla K(\rho,z-z')\,dz', \tag{2}$$

has an integrand dominated by a $1/R^3$ behavior. This behavior is canceled by letting

$$dz' = R_{\max}^3 \, du = \left[ \left( z - z' \right)^2 + \left( \rho + a \right)^2 \right]^{\frac{3}{2}} du \, , \tag{3}$$

or, upon integrating,

$$u = \frac{z' - z}{\left( \rho + a \right)^2 R_{\max}} = \frac{\Delta L \left( \xi_2 - \xi_2^0 \right)}{\left( \rho + a \right)^2 R_{\max}} \quad \text{and} \quad z' = z + \left( \rho + a \right)^2 R_{\max} \, u. \tag{4}$$

The use of (3) and (4) allows (2) to be rewritten as

$$\begin{aligned} I_1 &= \int_{u_{1L}}^{u_{1U}} B\left( \xi_1, \xi_2 \right) \nabla K\left( \rho, z - z^{(k)} \right) R_{\max}^3 \, du \\ &\approx \Delta L \sum_{k=1}^{K_1} \left[ \frac{w_k^{GL} \left( u_{1U} - u_{1L} \right) R_1^{(k)}}{\Delta L} \right] B\left( \xi_1^{(k)}, \xi_2^{(k)} \right) \nabla K\left( \rho, z - z^{(k)} \right), \end{aligned} \tag{5}$$

where

$$u_{1L} = -\frac{\Delta L \xi_2^0}{\left( \rho + a \right)^2 R_{\max}}, \quad u_{1U} = -\frac{\Delta L \max\left( \Delta \xi_1, -\xi_1^0 \right)}{\left( \rho + a \right)^2 R_{\max}}, \tag{6}$$

$$R_1^{(k)} = R_{\max}^3 = \left( \frac{\rho + a}{\sqrt{1 - \left[ u_1^{(k)} \left( \rho + a \right)^2 \right]^2}} \right)^3, \tag{7}$$

$$u_1^{(k)} = u_{1L} \xi_1^{GL(k)} + u_{1U} \xi_2^{GL(k)}, \quad z^{(k)} = z + \left( \rho + a \right)^2 R_{\max} \, u_1^{(k)}, \tag{8}$$

$$\xi_2^{(k)} = \xi_2^0 + \frac{\left( \rho + a \right)^2}{\Delta L} R_{\max} \, u_1^{(k)}, \ \left( \xi_1^{(k)} = 1 - \xi_2^{(k)} \right), \quad \Delta \xi_1 = \frac{\Delta z_1}{\Delta L} = \min\left( \xi_2^0, \Delta \xi \right) \tag{9}$$

and $\Delta \xi = a / \Delta L$ in this work. The integral $I_4$ is similarly evaluated.

The near-delta function behavior ($\rho$ near but not equal to $a$) present in the second integral $I_2$ is accounted for by letting

$$dz' = R_{\min}^2 \, du = \left[ \left( z - z' \right)^2 + \left( \rho - a \right)^2 \right] du \, , \tag{10}$$

which yields, after integrating,

$$u = \frac{1}{\rho - a} \tan^{-1} \left( \frac{z' - z}{\rho - a} \right) = \frac{1}{\rho - a} \tan^{-1} \left[ \frac{\Delta L \left( \xi_2 - \xi_2^0 \right)}{\rho - a} \right] \tag{11}$$

and

$$z' = z + \left( \rho - a \right) \tan\left[ \left( \rho - a \right) u \right]. \tag{12}$$

Hence, $I_2$ may now be written as

$$\begin{aligned} I_2 &= \int_{u_{2L}}^{u_{2U}} B\left( \xi_1, \xi_2 \right) \nabla K\left( \rho, z^{(k)} \right) R_{\min}^2 \, du \\ &\approx \Delta L \sum_{k=1}^{K_2} \left[ \frac{w_k^{GL} \left( u_{2U} - u_{2L} \right) R_2^{(k)}}{\Delta L} \right] B\left( \xi_1^{(k)}, \xi_2^{(k)} \right) \nabla K\left( \rho, z - z^{(k)} \right), \end{aligned} \tag{13}$$

where

$$u_{2L} = -\frac{1}{\rho - a}\tan^{-1}\left(\frac{\Delta L\,\Delta\xi_1}{\rho - a}\right),\;\; u_{2U} = 0, \tag{14}$$

$$R_2^{(k)} = R_{\min}^2 = \left(\rho - a\right)^2 \sec^2\left[\left(\rho - a\right)u_2^{(k)}\right], \tag{15}$$

$$u_2^{(k)} = u_{2L}\xi_1^{GL(k)} + u_{2U}\xi_2^{GL(k)}, \quad z^{(k)} = z + \left(\rho - a\right)\tan\left[\left(\rho - a\right)u_2^{(k)}\right], \tag{16}$$

and

$$\xi_2^{(k)} = \xi_2^0 + \frac{\left(\rho - a\right)}{\Delta L}\tan\left[\left(\rho - a\right)u_2^{(k)}\right],\; \left(\xi_1^{(k)} = 1 - \xi_2^{(k)}\right). \tag{17}$$

The integral $I_3$ is evaluated using the same approach as $I_2$.

The sample points $\xi_2^{(k)}$ are given in (9) and (17), while the bracketed quantities in (5) and (13), represent the new weights. These may be used in typical numerical quadrature routines.

## Results

The near field of a 1-meter wire dipole with a radius of 1 mm is calculated and compared with results using EIGER [3]. The dipole is modeled using 20 linear segments and lies on the *z* axis. It is exited at the center with a unit-strength voltage source at 300 MHz. The magnetic field is sampled 1 mm from the dipole surface and is shown in Figs. 1 and 2. There is good agreement between EIGER and the data generated using this formulation.

## Summary and Conclusions

A formulation for integrating the gradient of the thin wire kernel is presented. This approach employs a new expression for the gradient of the thin wire kernel derived from a recent technique for numerically evaluating the exact thin wire kernel. This approach should provide essentially arbitrary accuracy and may be used with higher-order elements and basis functions using the procedure described in [4].

## References


[1] D. R. Wilton and N. J. Champagne, "Evaluation and integration of the thin wire kernel," *IEEE Trans. Antennas Propagation*, vol. 54, no. 4, pp. 1200–1206, 2006.

[2] D. R. Wilton and N. J. Champagne, "Evaluating the gradient of the thin wire kernel," *2008 IEEE AP-S International Symposium and USNC/URSI Radio Science Meeting*, submitted.

[3] R. M. Sharpe, J. B. Grant, N. J. Champagne, W. A. Johnson, R. E. Jorgenson, D. R. Wilton, W. J. Brown, and J. W. Rockway, "EIGER: Electromagnetic Interactions GEneRalized," 1997 IEEE AP-S International Symposium and North American URSI Radio Science Meeting, Montreal, Canada, July 1997, pp. 2366–2369.

[4] N. J. Champagne, D. R. Wilton and J. D. Rockway, “The analysis of thin wires using higher-order elements and basis functions,” *IEEE Trans. Antennas Propagation*, vol. 54, no. 12, pp. 3815–3821, 2006.

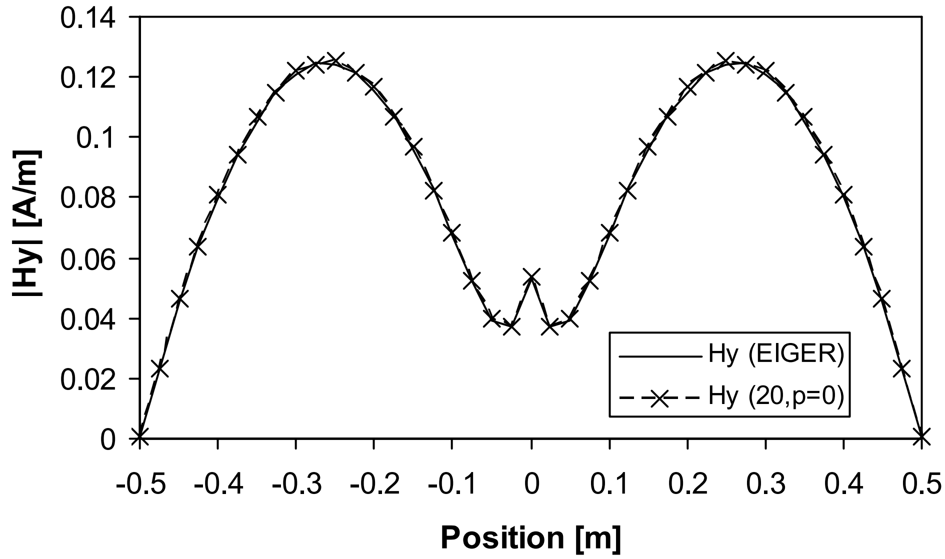


Fig. 1. The magnitude of the *y* component of the magnetic field 1 mm from the wire dipole.

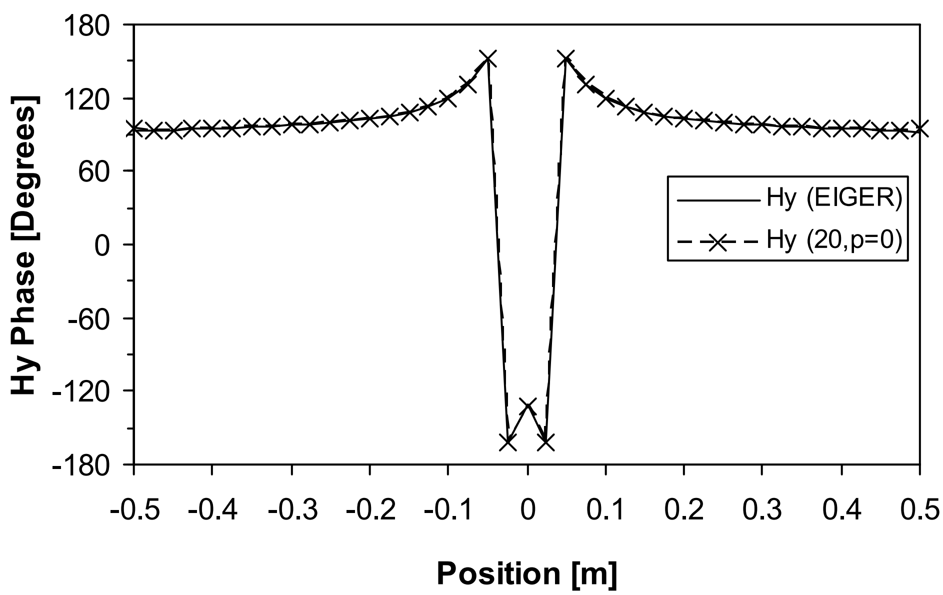


Fig. 2. The phase of the *y* component of the magnetic field 1 mm from the wire dipole.